Steady-State and Pre-Steady-State Kinetic Analysis of 8-Oxo-7,8-dihydroguanosine Triphosphate Incorporation and Extension by Replicative and Repair DNA Polymerases†

Heidi J. Einolf, Nathalie Schnetz-Boutaud, and F. Peter Guengerich*

Department of Biochemistry and Center in Molecular Toxicology, Vanderbilt University School of Medicine, Nashville, Tennessee 37232-0146

Received June 8, 1998; Revised Manuscript Received July 22, 1998

ABSTRACT: The kinetics of 8-oxo-7,8-dihydroguanosine triphosphate (8-oxo-dGTP) incorporation into DNA by *Escherichia coli* polymerases I exo$^-$ (KF$^-$) and II exo$^-$ (Pol II$^-$), HIV-1 RT reverse transcriptase (HIV-1 RT), and bacteriophage T7 exo$^-$ (T7$^-$) were examined to determine the misincorporation potential for 8-oxo-dGTP and to investigate the role of base pairing symmetry in DNA polymerase fidelity. 8-Oxo-dGTP was found to be a poor substrate for the four polymerases, with insertion efficiencies $>10^4$-fold lower than for dGTP incorporation. Insertion efficiencies of 8-oxo-dGTP were also consistently lower than for incorporation of dNTPs opposite template 8-oxo-G, previously studied in this laboratory. In steady-state reactions, T7$^-$ had a high preference for 8-oxo-dGTP insertion opposite A (97%) and HIV-1 RT, KF$^-$, and Pol II$^-$ preferred to insert 8-oxo-dGTP opposite C. Misinsertion frequencies for 8-oxo-dGTP also varied considerably from frequencies of misinsertion at template 8-oxo-G adducts for Pol II$^-$, HIV-1 RT, and T7$^-$. Pre-steady-state incorporation of 8-oxo-dGTP opposite C (but not opposite A) by HIV-1 RT, KF$^-$, and Pol II$^-$ displayed biphasic curves, with rates of initial incorporation 2- to 11-fold lower than normal dGTP incorporation. Although extension past template 8-oxo-G adducts had previously been shown to occur preferentially for the mispair, extension past primer 8-oxo-G:template A or C pairs was variable. The low and comparable estimated K_d values for dGTP and 8-oxo-dGTP binding to HIV-1 RT alone or HIV-1 RT·DNA complexes indicated that the initial binding was nonselective and had high affinity. The large difference (>3 orders of magnitude) in kinetic K_{dapp} values for 8-oxo-dGTP and dGTP binding to HIV-1 RT·DNA indicates that there are contributions to the kinetically determined K_{dapp} (such as conformational change and/or phosphodiester bond formation) which may be involved in the selection against 8-oxo-dGTP. The differences in binding (K_{dapp}), incorporation, and extension kinetics of 8-oxo-dGTP compared to normal dNTP incorporation at template 8-oxo-G adducts indicate that polymerase fidelity does not depend solely upon the overall geometry of Watson−Crick base pairs and reflects the asymmetry of the enzyme active site.

High fidelity of DNA replicative and repair polymerases is of paramount importance for the preservation of the genome. The replication of eukaryotic genomic DNA is an intricate process involving the assembly and control of many proteins. Simple DNA polymerase systems without proofreading activity, such as the repair enzymes *Escherichia coli* polymerase I (KF$^-$)[1] and Pol II$^-$[2] and the replicative polymerases T7$^-$ and HIV-1 RT, have been utilized to examine the catalytic mechanism of DNA replication and steps that ensure polymerase fidelity at DNA lesions. Kinetic studies of DNA polymerization utilizing these systems have contributed to the elucidation of a general mechanism of DNA polymerization (*4*).

Pre-steady-state kinetics have been used to examine enzyme single turnover cycles for these polymerases and have allowed characterization of the individual steps in the polymerization reaction (*5*−*8*). Steady-state kinetic analysis of DNA polymerization reactions can give information about the enzyme specificity but is limiting in that the individual rate constants are masked by the rates of enzyme/DNA association and disassociation (*4*). The general DNA polymerase mechanism consists of a series of steps beginning with the binding of the DNA to the enzyme, followed by dNTP binding to the enzyme/DNA complex. The binding of the dNTP induces a conformational change of the enzyme, which results in formation of a "tight" ternary complex (*7*). Phosphodiester bond formation occurs, followed by another

† This work was supported in part by United States Public Health Service (USPHS) Grants R35 CA44353 and P30 ES00267. H.J.E. was supported in part by USPHS Grant F32 CA75731.

* To whom correspondence should be addressed.

[1] Abbreviations: KF$^-$, *E. coli* polymerase I Klenow fragment exo$^-$; Pol II$^-$, *E. coli* polymerase II exo$^-$; T7$^-$, bacteriophage T7 DNA polymerase exo$^-$; HIV-1 RT, human immunodeficiency virus-1 reverse transcriptase; 8-oxo-dG, 8-oxo-7,8-dihydrodeoxyguanosine; 8-oxo-G, 8-oxo-7,8-dihydrodeoxyguanine; 8-oxo-dGTP, 8-oxo-7,8-dihydrodeoxyguanosine triphosphate; KF, *E. coli* polymerase I Klenow fragment exo$^+$; T7, bacteriophage T7 DNA polymerase exo$^+$; Tris, tris(hydroxymethyl)aminomethane; DTT, dithiothreitol; EDTA, (ethylenedinitrilo)tetraacetic acid; BSA, bovine serum albumin; A, adenine; C, cytosine; G, guanine.

[2] Pol II has been shown to be associated with DNA repair and the replication of chromosomal and episomal DNA (*1*−*3*).

S0006-2960(98)01346-4 CCC: $15.00
Published on Web 08/29/1998

conformational change allowing pyrophosphate release and translocation or release of the DNA.

Studies of correct dNTP incorporation by many polymerases, including KF$^-$, T7$^-$, and HIV-1 RT, have indicated that the first conformational change is rate-limiting and may be primarily involved in substrate selectivity (*5*−*7*). Kinetic studies of replication at DNA lesions, such as 8-oxo-G and O^6-methyldeoxyguanosine, indicated that chemistry (phosphodiester bond formation) is at least partially rate-limiting for both correct and incorrect incorporation by these polymerases, with the exception of HIV-1 RT (*8*−*10*). Formation of the phosphodiester bond also becomes partially rate-limiting during misincorporation reactions with KF and T7 (*11*, *12*). During misincorporations or replication at DNA lesions, the fidelity of a DNA polymerase appears to be compromised at specific steps in the polymerization pathway.

8-Oxo-G is a DNA lesion formed as a product of oxidative damage and is thought to be a major contributor to aging and cancer (*13*). In cells, 8-oxo-G can be formed by byproducts of aerobic metabolism, oxygen stress, radiation, toxins, and mutagens (*14*). Shibutani et al. (*15*) found that dATP and dCTP were incorporated opposite an 8-oxo-G lesion by KF, *E. coli* DNA polymerase I, HeLa cell DNA polymerases α and *β*, and calf thymus polymerase *δ* with varying efficiencies. In the case of KF, the insertion of dCTP was 7-fold in favor of dATP; however, the extension of the C:8-oxo-G pair was 12-fold less than an A:8-oxo-G pair. Pol *δ*, however, preferentially inserted dATP and efficiently extended the A:8-oxo-G pair. In a more detailed kinetic analysis of the misincorporation of dNTPs opposite 8-oxo-G by KF$^-$, Pol II$^-$, HIV-1 RT, and T7$^-$, dATP was misincorporated >30% of the time and all four enzymes were able to efficiently extend the mispair, but C:8-oxo-G base pairs were less efficiently extended (*8*, *9*). These in vitro misincorporation studies correlated well with the ability of 8-oxo-G to cause mainly G → T transitions in in vivo site specific mutagenesis assays in *E. coli* (*16*, *17*) and mammalian cells (*18*−*20*).

The biological importance of this lesion is substantiated by evidence of its time-dependent repair (*21*), urinary excretion (*22*), and the existence of repair enzymes specific for the elimination of 8-oxo-G lesions (*23*). In *E. coli*, two genes have been identified, mutations of which cause G:C → T:A transversions. One protein, MutM, possesses a DNA glycosylase activity that specifically removes 8-oxo-G from DNA, and the other protein, MutY, removes the A base from an A:8-oxo-G base pair (*24*−*28*). There also exists an enzyme (MutT) in *E. coli* and humans that specifically hydrolyzes 8-oxo-dGTP to the monophosphate (*29*, *30*). In *mutT*$^-$ strains of *E. coli*, the rates of A:T → C:G transversions are 10^3-fold over the wild-type strain, whereas mutation rates for *mutM*$^-$ and *mutY*$^-$ strains are only slightly higher than the wild-type strain (*31*). These studies suggest that the incorporation of 8-oxo-dGTP into DNA from the cellular nucleotide pool may have substantial importance for the mutagenicity of this lesion.

The potential of 8-oxo-dGTP to be misincorporated has been examined in vitro utilizing the α subunit of *E. coli* DNA polymerase III (*32*), KF$^-$, polymerase T4 exo$^-$, and *Thermus thermophilus* polymerase exo$^-$ (*33*); these polymerases incorporated 8-oxo-dGTP opposite both C and A. SV40 origin-dependent replication of double-stranded DNA in HeLa cell extracts containing 8-oxo-dGTP (*33*) indicated that 8-oxo-dGTP incorporation into DNA caused A → C transversions, which correlated with mutations found in *mutT*$^-$ strains of *E. coli* (*32*, *33*). Recently, 8-oxo-dGTP has been found to be mutagenic in *E. coli* cells and has been found to similarly contribute to the formation of 8-oxo-G in DNA as well as directly oxidized DNA (*31*, *34*).

The purpose of this study was to examine the misincorporation of 8-oxo-dGTP with the model DNA polymerases KF$^-$, Pol II$^-$, HIV-1 RT, and T7$^-$ by steady-state and pre-steady-state kinetics. The kinetic parameters were then compared to previous complementary studies of normal dNTP incorporation opposite template 8-oxo-G (*8*, *9*) to determine whether overall base-pair geometry is the dominant factor in DNA polymerase fidelity at 8-oxo-G adducts. It has been hypothesized that geometrical properties of the enzyme active site and overall Watson−Crick geometry of the newly formed base pair dominate nucleotide insertion specificity (*4*, *35*). In contrast, the fidelity of a DNA polymerase has been shown to differ depending upon whether the base is in the template or as the dNTP for mispairs involving the same two bases (*36*−*38*).

EXPERIMENTAL PROCEDURES

Synthesis of 8-Oxo-dGTP. 8-Oxo-dG (**6**, Scheme 1) was prepared from 7,8-dihydro-N^2-isobutyryl-8-oxo-2′-deoxyguanosine (**5**), an intermediate in the synthesis of 8-oxo-dG phosphoroamidite, previously prepared in our laboratory from deoxyguanosine (**1**) as described (*8*, *39*). Treatment of **5** (100 mg) with 1 mL of concentrated aqueous NH_4OH and 7 μL of 2-mercaptoethanol at 55 °C for 16 h resulted in the removal of the isobutyryl moiety to produce 8-oxo-dG. 8-Oxo-dGTP was synthesized from 8-oxo-dG according to the method of Ludwig (*40*). 8-Oxo-dG (100 mg) was dried 3× by the addition of 2 mL of anhydrous pyridine, and the solvent was evaporated in vacuo with stirring for a minimum of 8 h after each addition of pyridine. All reactants were anhydrous and added to the reaction under dry Ar using dried syringes. To the anhydrous 8-oxo-dG, 2 mL of trimethyl phosphate and 60 μL of $POCl_3$ were added and the mixture was stirred for 4 h at −20 °C. The product, 7,8-dihydro-N^2-8-oxo-2′-deoxyguanosine 5′-phosphorodichloridate (**7**), was reacted with 200 μL of tributylamine and 1.0 g of tributylammonium pyrophosphate in 5 mL *N*,*N*-dimethylformamide for 30 min at −20 °C. The reaction was taken to room temperature for 10 min, and the product **8** was hydrolyzed by the addition of 5 mL of 2 M $(C_2H_5)_3NH_2CO_3$ buffer, pH 7.5. 8-Oxo-dGTP was washed 3 times with an equal volume of $(C_2H_5)_2O$ and dried by lyophilization after the addition of H_2O. 8-Oxo-dGTP was purified by SAX-HPLC on a 5 μm, 9.4 × 250 mm Partisil SAX column (Phenomenex, Torrance, CA) by isocratic elution (2 mL min^{-1}) for 5 min with a mixture (v/v) of 0.20 M KH_2PO_4 and 20% CH_3CN (buffer A), followed by elution with a linear gradient of buffer A to 0.20 M KH_2PO_4, 20% CH_3CN (v/v), and 1.0 M NaCl (buffer B) over 60 min and further isocratic elution with buffer B for 5 min. The 8-oxo-dGTP peak was collected, dried by lyophilization, and dissolved in H_2O. 8-Oxo-dGTP was passed through two (tandem) 5 μm reverse-phase HPLC columns equilibrated with H_2O and eluted with H_2O (Beckman Ultrasphere ODS RP, 10 × 250 mm, 1 mL min^{-1}) to remove salts. Subsequently, the 8-oxo-dGTP

Scheme 1: Synthesis of 8-oxo-dGTP (*39*, *40*)

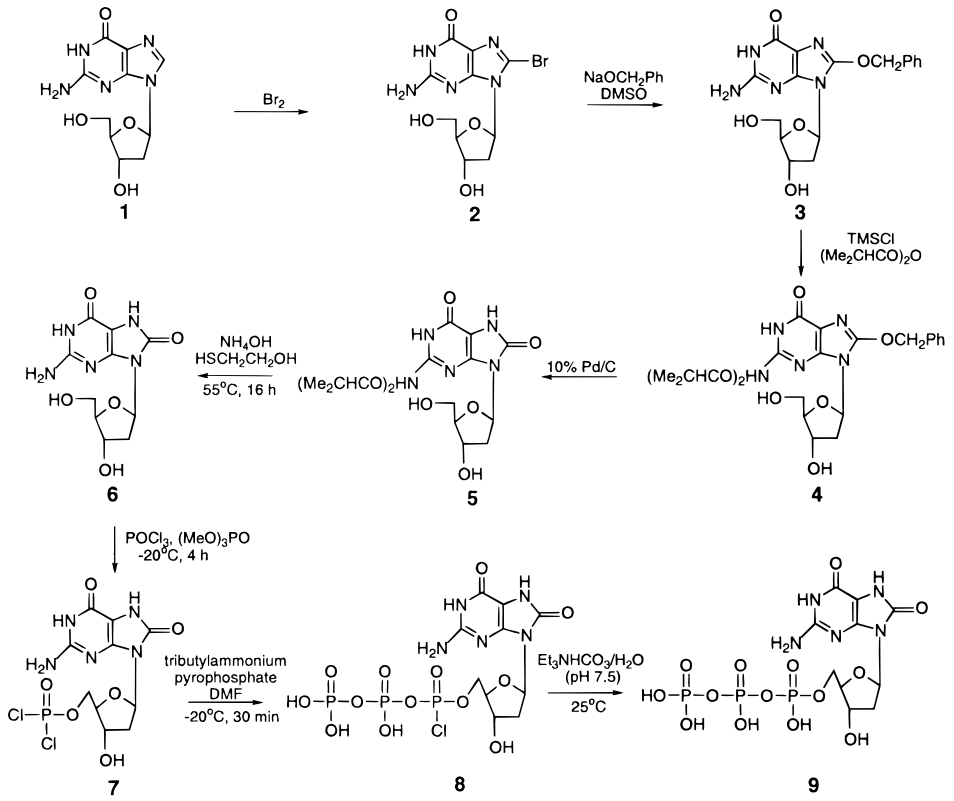

product was passed through a 1.5 × 5 cm Chelex 100 column (Bio-Rad, Hercules, CA) to remove metal ions, which interfered with the ^{31}P NMR spectra. The column was equilibrated with 50 mL of H_2O, and the 8-oxo-dGTP was eluted at 1 mL min^{-1} with H_2O (detection by UV at 293 nm). ^{31}P NMR analysis of the eluted 8-oxo-dGTP showed contamination from di- and monophosphates. NMR spectra were recorded on a Bruker 300 AN spectrophotometer operating at 121.4 Hz (^{31}P). Chemical shift values (δ) are reported relative to H_3PO_4 (85%) for ^{31}P NMR (external standard). ^{31}P NMR (D_2O): triphosphate, δ −5.11 (d, $J_{\gamma-\beta}$ = 20.1 Hz, P_γ), −9.86 (d, $J_{\alpha-\beta}$ = 19.2 Hz, P_α), −20.67 (t, P_β); diphosphate, δ −5.25 (d, $J_{\alpha-\beta}$ = 21.8 Hz, P_β), −9.52 (d, P_α); monophosphate, δ −6.46 (d, P_α). To eliminate the breakdown of 8-oxo-dGTP, the sample eluted from the Chelex 100 column was purified once by DEAE-HPLC (Phenomenex, 5 μm, 300 Å, 10 × 250 mm) utilizing volatile buffers. 8-Oxo-dGTP was purified from contaminating mono- and diphosphates by isocratic elution at a flow rate of 2 mL min^{-1} for 5 min with 50 mM NH_4HCO_3, pH 6.0 (buffer C) followed by elution with a linear gradient of C to 200 mM NH_4HCO_3, pH 6.0 (buffer D) over 60 min and isocratic elution with D for 5 min (see Supporting Information). Standard dGDP and dGTP were completely separated utilizing the same elution conditions. The 8-oxo-dGTP peak was collected and lyophilized several times after the addition of H_2O to remove the salt. The concentration of 8-oxo-dGTP was determined utilizing the extinction coefficient for 8-oxo-dG in H_2O, ϵ_{293} = 10 300 M^{-1} cm^{-1} (*41*). The identity and purity of 8-oxo-dGTP was confirmed by electrospray positive-ion mass spectrometry in the Vanderbilt facility (*m*/*z*): calcd for MH^+, 524; found, 524.4 (see Supporting Information).

Table 1: Oligonucleotides Utilized in These Studies

12 mer	**5'- GGCGTCTGCGTC**
16C mer	**3'- CCGCAGACGCAGCGAG**
16A mer	**3'- CCGCAGACGCAGAGAG**
24 mer	**5'-** CGGAGCTCGGTC**GGCGTCTGCGTC**
36C mer	**3'-** GCCTCGAGCCAG**CCGCAGACGCAGCGAG**GACGCCGA
36A mer	**3'-** GCCTCGAGCCAG**CCGCAGACGCAGAGAG**GACGCCGA
13 mer	**5'- GGCGTCTGCGTCG***
25 mer	**5'-** CGGAGCTCGGTC**GGCGTCTGCGTCG***

G* = 8-oxo-G

Oligonucleotides. The sequences of oligonucleotides chosen for these studies were complementary to those used previously in our laboratory (*8*, *9*) to examine normal dNTP incorporation into DNA templates containing 8-oxo-G (Table 1). The 12-mer, 16C-mer, and 16A-mer oligonucleotides were synthesized previously in our laboratory as described (*8*). The oligonucleotides were purified by reversed-phase HPLC utilizing a 10 × 250 mm, 5 μm YMC-Pack ODS-AQ column (YMC, Wilmington, NC). The elution gradient was as follows: 100% 50 mM NH_4HCO_2, pH 6.2 (buffer E) to 70% E; 30% CH_3OH, v/v (buffer F) over 40 min, 70% E; 30% F (v/v) to 50% E; 50% F (v/v) over 10 min, followed by regeneration of the column to 100% E over 10 min. The oligonucleotides were lyophilized several times, repeating after the addition of H_2O. The purity of the oligonucleotides were confirmed by capillary gel electrophoresis using a Beckman P/ACE 2000 instrument (Beckman, Fullerton, CA) with a ssDNA 100-R gel-filled 57 cm × 100 μm capillary. The oligonucleotides were applied at 5 kV for 1 s at 30 °C and separated at 10 kV with a Tris−borate−urea buffer supplied by the manufacturer.

The 23-mer, 24-mer, 36C-mer, 36A-mer, and oligonucleotides containing a 3′ 8-oxo-G (13-mer and 25-mer) were purchased from Midland Certified Reagent Co. (Midland, TX). The 3′ 8-oxo-G-containing oligonucleotides were purchased with a 3′-phosphate group, which was removed with phosphatase. The oligonucleotide (1.5 A_{260} units $\approx$ 300 pmol) was treated with 4 U of calf intestinal phosphatase (Promega, Madison, WI) in 50 mM Tris-HCl (pH 9.3, 25 °C) buffer containing 1 mM $MgCl_2$, 0.1 mM $ZnCl_2$, and 1 mM spermidine at 37 °C for 30 min. An additional 4 U of phosphatase was added to the reaction and incubated for another 1.5 h at 37 °C. The reaction was stopped by heating at 75 °C for 10 min, and the oligonucleotides were concentrated and desalted utilizing Micron microconcentrators (Amicon, Beverly, MA) as described by the manufacturer. The 13-mer and 25-mer oligonucleotides were purified by denaturing polyacrylamide gel electrophoresis [20% acrylamide (w/v), 1.5% bisacrylamide (w/v), 8.0 M urea]. The 24-mer and 36-mer oligonucleotides were purified by a 16% denaturing polyacrylamide gel electrophoresis [16% acrylamide (w/v), 1.5% bisacrylamide (w/v), 8.0 M urea]. The oligonucleotides were excised from the gel, crushed, and eluted with H_2O at 4 °C for 15 h with shaking. The DNA was isolated and desalted utilizing Micron microconcentrators. The purity of the oligonucleotides was confirmed by capillary gel electrophoresis using a Beckman P/ACE 5000 instrument with an eCAP ssDNA 100-R gel-filled 27 cm $\times$ 100 μm P/ACE eCAP capillary. The oligonucleotides were applied at 10 kV for 10 s at 30 °C and separated at 11 kV with the Tris−borate−urea buffer supplied by the manufacturer.

The concentrations of the oligonucleotides were determined by UV absorbance utilizing extinction coefficients calculated by the method of Borer (*42*): 12-mer, ϵ_{260} = 105 100 M^{-1} cm^{-1}; 13-mer, ϵ_{260} = 115 700 M^{-1} cm^{-1}; 16C-mer, ϵ_{260} = 154 500 M^{-1} cm^{-1}; 16A-mer, ϵ_{260} = 161 100 M^{-1} cm^{-1}; 23-mer, ϵ_{260} = 204 900 M^{-1} cm^{-1}; 24-mer, ϵ_{260} = 213 700 M^{-1} cm^{-1}; 25-mer, ϵ_{260} = 224 300 M^{-1} cm^{-1}; 36C-mer, ϵ_{260} = 341 900 M^{-1} cm^{-1}; 36A-mer, ϵ_{260} = 348 300 M^{-1} cm^{-1}.

End-Labeling of Primer and Primer/Template Annealing. The 12-mer, 13-mer, 24-mer, and 25-mer primer oligonucleotides were 5′ end-labeled with [γ-^{32}P]dATP (3000 Ci/mmol) and T4 polynucleotide kinase. Unreacted [γ-^{32}P]ATP was separated from labeled oligonucleotides with Bio-spin 6 chromatography columns (Bio-Rad). The 12-mer or 13-mer labeled primers were annealed to 16C-mer or 16A-mer templates in a ratio of 1:1.5 (primer:template) in a final concentration of 50 mM Tris-HCl buffer (pH 7.4) containing 5 mM $MgCl_2$, 2 mM 2-mercaptoethanol, 100 nM primer, and 150 nM template for steady-state assays (250 nM for pre-steady-state rapid-quench assays). The 24-mer or 25-mer labeled primers were annealed to the 36C-mer or 36A-mer templates in a ratio of 1:1.5 (primer:template), as described previously (*8*, *9*), for a final concentration of 250 nM primer/template.

Enzymes. KF^-, Pol II^-, $T7^-$, and HIV-1 RT enzymes utilized in these studies were expressed and purified previously in this laboratory (*8*, *9*). Protein concentrations were estimated with ϵ_{280} values of 63.2 mM^{-1} cm^{-1} for KF^-, 128 mM^{-1} cm^{-1} for Pol II^-, 144 $mM^{-1}cm^{-1}$ for $T7^-$, 13.7 mM^{-1} cm^{-1} for thioredoxin, and 520 mM^{-1} cm^{-1} for HIV-1 RT heterodimer.[3]

Steady-State Reactions. KF^- or Pol II^- was diluted in 500 mM Tris-HCl buffer (pH 7.4) containing 50 mM $MgCl_2$ and 10 mM EDTA. The annealed 12/16-mer or 13/16-mer primer:template was mixed with the diluted enzyme in a 4:1 ratio (primer/template to enzyme). The reactions were initiated with the addition of an equal volume of 100 mM Tris-HCl (pH 7.4) containing 25 mM $MgCl_2$ (buffer G) and 2$\times$ dNTP at varying concentrations in a total reaction volume of 8 μL to yield final concentrations of 120 mM Tris·HCl (pH 7.4), 20 mM $MgCl_2$, 1 mM EDTA, 0.8 mM 2-mercaptoethanol, and 40 nM primer/template.

HIV-1 RT was diluted in a buffer containing 500 mM Tris-HCl (pH 7.4) and 500 mM NaCl. The annealed 24/36-mer or 25/36-mer was mixed with the diluted enzyme in a 4:1 ratio (primer/template to enzyme). The reactions were initiated with the addition of an equal volume of buffer G containing varying concentrations of 2$\times$ dNTP in a total reaction volume of 8 μL to yield final concentrations of 120 mM Tris·HCl (pH 7.4), 50 mM NaCl, 14.5 mM $MgCl_2$, 0.8 mM 2-mercaptoethanol, and 100 nM primer/template.

$T7^-$ was diluted to 1.0 μM in a buffer containing 400 mM Tris·HCl (pH 7.4), 10 mM EDTA, and 500 mM NaCl (buffer H). DTT was added to 2.5 μL of thioredoxin and diluted with buffer H to give a concentration of 10 μM thioredoxin and 5 mM DTT. $T7^-$ and thioredoxin were combined in a molar ratio of 1:20 ($T7^-$:thioredoxin) in buffer H with 10 mM DTT and 1 mg BSA mL^{-1}. The annealed 24/36-mer or 25/36-mer was mixed with the diluted enzyme in a 4:1 ratio (primer/template to enzyme). The reactions were initiated with the addition of an equal volume of buffer G containing varying concentrations of 2$\times$ dNTP in a total reaction volume of 8 μL to yield final concentrations of 110 mM Tris·HCl (pH 7.4), 1 mM EDTA, 50 mM NaCl, 0.8 mM DTT, 0.07 mg BSA mL^{-1}, 14.5 mM $MgCl_2$, 0.8 mM 2-mercapthoethanol, and 100 nM primer/template.

The steady-state reactions with KF^- utilized 0.2 nM enzyme for dGTP incorporation into 12/16C-mer, 35 nM KF^- for 8-oxo-dGTP incorporation into 12/16C-mer, and 2 nM KF^- for 8-oxo-dGTP incorporation into 12/16A-mer. The reactions with Pol II^- utilized 0.7 nM enzyme for dGTP incorporation into 12/16C-mer, 13 nM Pol II^- for 8-oxo-dGTP incorporation into 12/16C-mer, and 17 nM Pol II^- for 8-oxo-dGTP incorporation into 12/16A-mer. Reactions with HIV-1 RT utilized 3.5 nM enzyme for dGTP incorporation into 24/36C-mer, 13 nM HIV-1 RT for 8-oxo-dGTP incorporation into 24/36C-mer, and 11 nM HIV-1 RT for 8-oxo-dGTP incorporation into 24/36A-mer. For reactions with $T7^-$, 0.55 nM enzyme was utilized for dGTP incorporation into 24/36C-mer, 15 nM $T7^-$ for 8-oxo-dGTP incorporation into 24/36C-mer, and 11 nM $T7^-$ for 8-oxo-dGTP incorporation into 24/36A-mer.

The steady-state reactions with KF^- and $T7^-$ were run at 25 °C, and those with Pol II^- and HIV-1 RT, at 37 °C (*8*, *9*). All the steady-state reactions were run in triplicate, and the reactions (8 μL reaction volume) were quenched with 16 μL of 20 mM EDTA, pH 7.4. The products were

[3] The HIV-1 RT extinction coefficient value was determined by Dr. L. L. Furge (this laboratory) by quantitative amino acid analysis.

separated by denaturing polyacrylamide gel electrophoresis [16% acrylamide (w/v), 1.5% bisacrylamide (w/v), 8.0 M urea], and the amount of primer extended was quantitated utilizing a Molecular Dynamics model 400E phosphorimager (Molecular Dynamics, Sunnyvale, CA) and Image Software version 3.3. The k_{cat} and K_m values were determined by nonlinear regression using the k·cat computer program (Biometallics, Princeton, NJ).

Pre-Steady-State Kinetics. Pre-steady-state rapid-quench experiments were performed utilizing a KinTek Quench Flow Apparatus (model RQF-3, KinTek Corp., State College, PA). Reactions were initiated by rapid mixing of dNTP in buffer G with a primer/template/enzyme solution. The final concentrations of the reactants were 100 nM primer/template and $^1/_2$ the concentration of the enzyme diluting buffers utilized in steady-state reactions. The reactions were quenched with equal volumes of 0.6 M EDTA at times varying from 5 ms to 10 s. The products were analyzed as described for steady-state assays. The k_{pol} (maximum rate of nucleotide incorporation) was determined by a single-exponential analysis of a plot of $\ln(P_n - P_t)$ versus t to yield a line with slope $-k_{obs}$, where P_n is the concentration of product at the end of the burst phase and P_t is the concentration of product at time t. Graphically, the data was fit to the burst equation $y = A(1 - e^{-k_p t}) + k_{ss}t$, where A = burst amplitude, k_p = pseudo-first-order rate constant, t = time, and k_{ss} = steady-state rate of nucleotide incorporation.

Next Correct Base Pair Extension following 8-Oxo-dGTP Incorporation. Steady-state assays of the next correct base insertion (dCTP) after 8-oxo-dGTP incorporation were performed as described above. The reactions with KF^- utilized 1.3 nM enzyme for dCTP incorporation into 13/16C-mer and 0.7 nM KF^- for dCTP incorporation into 13/16A-mer. The reactions with Pol II^- utilized 5.8 nM enzyme for dCTP incorporation into 13/16C-mer and 1.7 nM Pol II^- for dCTP incorporation into 13/16A-mer. For reactions with HIV-1 RT, 6.1 nM enzyme was utilized for dCTP incorporation into 25/36C-mer and 5.9 nM HIV-1 RT for dCTP incorporation into 25/36A-mer. For reactions with $T7^-$, 2.8 nM enzyme was utilized for dCTP incorporation into 24/36C-mer and 0.4 nM $T7^-$ for dCTP incorporation into 25/36A-mer.

Pre-steady-state rapid-quench analysis of dCTP incorporation after 8-oxo-dGTP incorporation was performed as described above.

K_d Determination of dGTP or 8-Oxo-dGTP Binding to HIV-1 RT. The thermodynamic equilibrium K_d for dNTP binding to HIV-1 RT was estimated by titration of dGTP or 8-oxo-dGTP (0.0013−1.3 μM) into a solution containing 40 nM HIV-1 RT, 75 mM Tris-HCl (pH 7.4), 6.2 mM $MgCl_2$, and 50 mM NaCl (final concentrations), and intrinsic tryptophan fluorescence was measured with a Varian SF-330 spectrofluorometer (290 nm excitation, 338 nm emission, Varian, Walnut Creek, CA) as described previously (*43*). The data were fit to a fluorescence quadratic equation to estimate a K_d: $E{\cdot}dNTP = F_o + (A/E_t)(0.5)[(K_d + E_t + dNTP_t) - [(K_d + E_t + dNTP_t)^{2-4{\cdot}Et{\cdot}dNTPt}]^{1/2}]$, where F_o = initial observed fluorescence intensity, A = amplitude, E_t = [total enzyme], $dNTP_t$ = [total dNTP], and K_d = dissociation constant for the reaction $E + dNTP \leftrightarrow E{\cdot}dNTP$.

K_d Determination of dGTP or 8-Oxo-dGTP Binding to HIV-1 RT·DNA. The equilibrium dissociation constant for dGTP or 8-oxo-dGTP binding to HIV-1 RT·dideoxy-terminated primer/template complexes was also determined by intrinsic tryptophan fluorescence quenching. A 23-mer oligonucleotide was annealed to the 36A-mer template in a final concentration of 50 mM Tris-HCl buffer (pH 7.4), 5 mM $MgCl_2$, 2 mM 2-mercaptoethanol, 0.4 mM primer, and 0.6 mM template. The 24-mer dideoxy-terminated primer was prepared by incubating the annealed 23/36A-mer with KF^- and ddCTP in a system containing final concentrations of 20 μM KF^-, 1 mM ddCTP, 125 mM Tris-HCl (pH 7.4), 20 mM $MgCl_2$, 1 mM 2-mercaptoethanol, 1 mM EDTA, and 0.2 mM 23/36A-mer for 1 h at 37 °C. The reaction was desalted by Microcon microconcentrators, and the 24-mer dideoxy-terminated primer (24ddC-mer) was isolated by denaturing polyacrylamide gel electrophoresis. The purity of the 24ddC-mer was confirmed by capillary gel electrophoresis and annealed to the 36C-mer template in a 1:1 ratio, as described above. dGTP or 8-oxo-dGTP (0.0013−1.3 μM) was titrated into a solution of 40 nM HIV-1 RT, 100 nM 24ddC/36C-mer, 85 mM Tris-HCl (pH 7.4), 7.2 mM $MgCl_2$, 0.4 mM 2-mercaptoethanol, and 50 mM NaCl (final concentrations). Binding of the triphosphate to HIV-1 RT·24ddC/36C-mer complexes was determined by steady-state tryptophan fluorescence quenching, and the K_d was determined as described above.

The kinetic K_{dapp} value for dGTP or 8-oxo-dGTP binding to HIV-1 RT·primer/template complexes was estimated by pre-steady-state rapid-quench analysis. The dNTP concentration dependence of the pre-steady-state burst rates was examined by varying the concentration of dGTP or 8-oxo-dGTP and measuring the pre-steady-state burst rates of dNTP incorporation into 24/36C primer/template complexes. The values of k_{pol} were determined by single-exponential analysis as described above. The pre-steady-state rates were plotted against [dNTP], and the data were fit to the hyperbola $k_{obs} = [k_{pol}[dNTP]/([dNTP] + K_{dapp})]$ to determine K_{dapp} (*44*).

RESULTS

Steady-State Kinetics of dGTP Incorporation Opposite Template C and 8-Oxo-dGTP Incorporation Opposite Template C or A. The selectivities of the polymerases were examined for 8-oxo-dGTP incorporation in comparison to normal dNTP insertion opposite 8-oxo-G in template DNA, previously studied in this laboratory (*8*, *9*). Due to similarities in base pairing geometry of 8-oxo-dGTP:A or 8-oxo-dGTP:C pairs with dATP:8-oxo-G or dCTP:8-oxo-G pairs, the insertion efficiencies (k_{cat}/K_m) and misinsertion frequencies, determined by the relationship $f = (k_{cat}/K_m)_A/(k_{cat}/K_m)_C$ (*45*), of the polymerases should be similar if the maintenance of overall Watson−Crick geometry of the two bases in the enzyme active site is a dominant factor for polymerase fidelity.

Steady-state parameters for dGTP incorporation opposite C and 8-oxo-dGTP incorporation opposite C or A by KF^-, Pol II^-, HIV-1 RT, and $T7^-$ are shown in Table 2. The correct insertion of 8-oxo-dGTP opposite C was preferred by the DNA repair polymerase KF^-, and selectivity against the incorrect incorporation of 8-oxo-dGTP was largely influenced by k_{cat} rather than K_m values. The k_{cat} value for the insertion of 8-oxo-dGTP opposite C by KF^- was 38-fold lower than the k_{cat} value of the incorporation of dGTP,

Table 2: Steady-State Kinetic Parameters for the Incorporation of 8-Oxo-dGTP

dNTP:template base	K_m (mM)	k_{cat} (min^{-1})	k_{cat}/K_m (mM^{-1} min^{-1})[a]	f[b]	% misincorporation[c]
KF$^-$					
dGTP:C	0.00 070 ± 0.000 11	12 ± 0.5	17 000		
8-oxo-dGTP:C	2.9 ± 0.6	0.32 ± 0.02	0.11		
8-oxo-dGTP:A	0.033 ± 0.011	0.0016 ± 0.0002	0.048	0.44	31
Pol II$^-$					
dGTP:C	0.000 87 ± 0.000 25	4.2 ± 0.4	4 800		
8-oxo-dGTP:C	3.9 ± 0.6	0.059 ± 0.004	0.015		
8-oxo-dGTP:A	9.6 ± 5.7	0.0064 ± 0.0023	0.00067	0.045	4
HIV-1 RT					
dGTP:C	0.000 30 ± 0.000 07	1.8 ± 0.1	6 000		
8-oxo-dGTP:C	1.7 ± 0.4	0.44 ± 0.04	0.26		
8-oxo-dGTP:A	2.2 ± 0.2	0.28 ± 0.01	0.13	0.50	33
T7$^-$					
dGTP:C	0.001 9 ± 0.000 4	4.4 ± 0.4	2 300		
8-oxo-dGTP:C	15 ± 5	0.010 ± 0.002	0.000 67		
8-oxo-dGTP:A	13 ± 0.8	0.27 ± 0.01	0.021	31	97

[a] Frequency of 8-oxo-dGTP insertion. [b] Apparent misinsertion frequency, defined as $f = [(k_{cat}/K_m)_A/(k_{cat}/K_m)_C]$. [c] Estimated % misincorporation $= (f/1 + f) \times 100$.

whereas the k_{cat} value for the misincorporation of 8-oxo-dGTP opposite A was 7500-fold lower. The K_m values for 8-oxo-dGTP incorporation opposite C and A were 4100- and 47-fold greater, respectively, than for dGTP incorporation opposite C. These steady-state parameters were utilized to determine a misinsertion frequency (f) value of 0.44 for 8-oxo-dGTP incorporation by KF, which predicts a 31% misincorporation of 8-oxo-dGTP opposite A.

Pol II$^-$ also preferred to correctly insert 8-oxo-dGTP opposite C. Steady-state kinetic parameters for 8-oxo-dGTP incorporation by Pol II$^-$ predicted a low misinsertion frequency of 0.045, which corresponds to a 4% misincorporation for 8-oxo-dGTP opposite A (Table 2). This low misincorporation frequency was defined by a low steady-state rate and a high K_m value for 8-oxo-dGTP misincorporation. The k_{cat} values for the incorporation of 8-oxo-dGTP opposite C and A were 71- and 660-fold lower than the k_{cat} value for insertion of dGTP opposite C. The K_m values were 500- and 11 000-fold greater for 8-oxo-dGTP incorporation opposite C and A, respectively, than for dGTP incorporation opposite C.

HIV-1 RT selectivity against 8-oxo-dGTP incorporation opposite C or A was influenced more by K_m than k_{cat} values. The K_m values for 8-oxo-dGTP incorporation opposite C and A were 5700- and 7300-fold greater, respectively, than for unmodified dGTP incorporation opposite C. The steady-state rates (k_{cat}) of 8-oxo-dGTP incorporation opposite C and A by HIV-1 RT only differed by 4- and 6-fold, respectively, from the rates of dGTP insertion opposite C (Table 2). HIV-1 RT also preferentially inserted 8-oxo-dGTP opposite C, with a misinsertion frequency of 0.50, which predicts a misincorporation of 33%.

The DNA polymerase that had the highest frequency of 8-oxo-dGTP misincorporation ($f = 31$) was the replicative DNA polymerase, T7$^-$ (Table 2). The high misincorporation (97%) of 8-oxo-dGTP by T7$^-$ was characterized by a 27-fold higher k_{cat} for the misincorporation reaction than for the correct incorporation and similar K_m values for both the correct and incorrect insertion of 8-oxo-dGTP (13 and 15 mM). In comparison to the insertion of dGTP opposite C, the steady-state rate of 8-oxo-dGTP misincorporation was only 16-fold lower than dGTP incorporation opposite C; for the correct incorporation of 8-oxo-dGTP the k_{cat} value was 440-fold lower. The K_m values for 8-oxo-dGTP incorporation opposite C and A relative to dGTP incorporation opposite C were similar (7900- and 6800-fold greater, respectively).

Pre-Steady-State Rapid-Quench Kinetics of dGTP Insertion Opposite C and 8-Oxo-dGTP Incorporation Opposite Template C or A. Pre-steady-state analysis of 8-oxo-dGTP insertion was performed to measure the rate of nucleotide incorporation in single turnover reactions, to eliminate any interfering rates of enzyme/DNA association and dissociation. Pre-steady-state (rapid-quench) progress curves for 8-oxo-dGTP incorporation opposite C or A and dGTP incorporation opposite C are shown in Figures 1 and 2. A single turnover of the enzyme occurred within 0.1 s for the correct incorporation of unmodified dGTP for all enzymes studied. Incorporation of 8-oxo-dGTP, however, never reached complete enzyme turnover, resulting in substoichometric bursts (product:enzyme).

Pre-steady-state incorporation of dGTP and 8-oxo-dGTP by KF$^-$ is shown in Figure 1A,B. The k_{pol} (maximum rate of nucleotide addition) for normal dGTP incorporation was determined to be 780 min^{-1} as determined by single-exponential analysis. The incorporation of 8-oxo-dGTP opposite C by KF$^-$ demonstrated an initial burst of 8-oxo-dGTP incorporation with a rate of 260 min^{-1}, 3-fold lower than normal dGTP incorporation. There was no initial burst of 8-oxo-dGTP incorporation opposite A (rate of 8-oxo-dGTP misincorporation of 0.067 min^{-1}).

The k_{pol} determined from the pre-steady-state progress curve for dGTP incorporation opposite C by Pol II$^-$ was determined to be 3300 min^{-1} (Figure 1C). The pre-steady-state reaction curves of 8-oxo-dGTP incorporation opposite C and A by Pol II$^-$ (Figure 1D) resembled that of KF$^-$, with a more rapid incorporation of 8-oxo-dGTP opposite C than A. The burst rate of 8-oxo-dGTP incorporation opposite C was determined to be 290 min^{-1}, 11-fold lower than dGTP incorporation by Pol II$^-$ opposite C. As with KF$^-$, no burst of 8-oxo-dGTP incorporation opposite A was observed ($k = 0.0078$ min^{-1}).

Pre-steady-state incorporation of dGTP and 8-oxo-dGTP by HIV-1 RT is shown in Figure 2A,B. The burst rate (k_{pol})

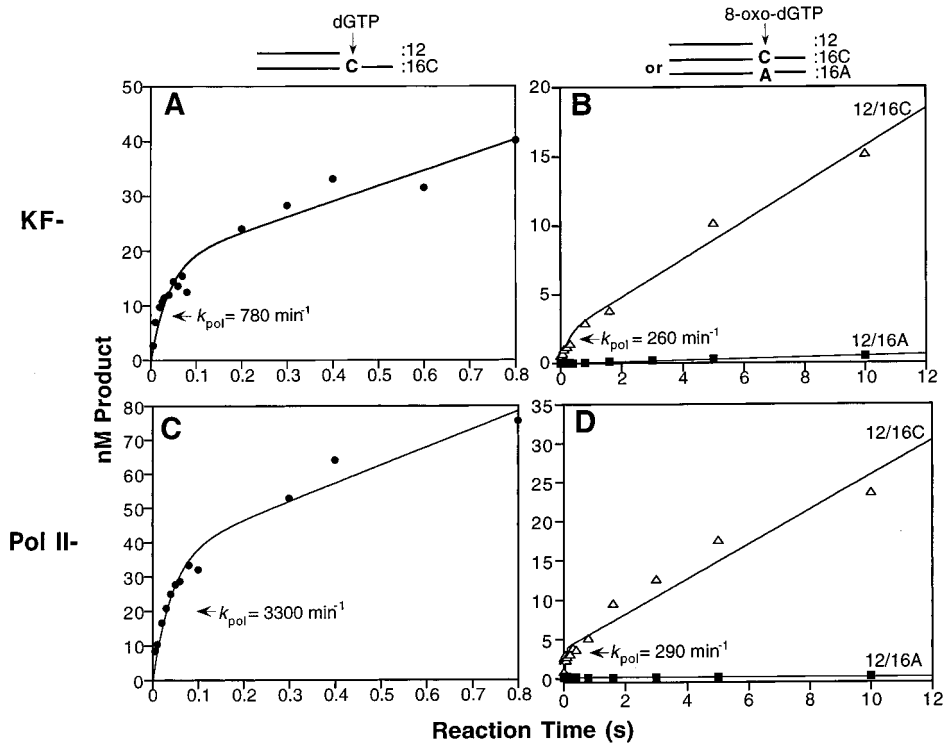

FIGURE 1: Pre-steady-state rapid-quench kinetics of nucleotide incorporation. (A) KF$^-$ (34 nM) was incubated with 100 nM 12/16C-mer and mixed with a solution of dGTP (60 μM) in the rapid-quench instrument. All the reactions were quenched at specified times with a final concentration of 0.3 M EDTA (●). (B) KF$^-$ (35 nM) was incubated with 100 nM 12/16C-mer (△) or 46 nM KF$^-$ with 100 nM 12/16A-mer (■), mixed with a solution of 8-oxo-dGTP (5 mM), and quenched at various times with EDTA. (C) Pol II$^-$ (18 nM) was incubated with 100 nM 12/16C-mer, mixed with a solution of dGTP (60 μM), and quenched at various times with EDTA (●). (D) Pol II$^-$ (40 nM) was incubated with 100 nM 12/16C-mer (△), or 37 nM Pol II$^-$ with 100 nM 12/16A-mer (■), mixed with a solution of 8-oxo-dGTP (5 mM), and quenched at various times with EDTA.

for dGTP incorporation opposite C was determined to be 2000 min^{-1}. The incorporation of 8-oxo-dGTP opposite C showed a burst of product formation with a k_{pol} value of 900 min^{-1}, 2-fold lower than correct dGTP incorporation (Figure 2B). Little incorporation of 8-oxo-dGTP opposite A (k = 0.23 min^{-1}) was observed.

The rate of the pre-steady-state burst for dGTP incorporation opposite C by T7$^-$ was determined to be 1700 min^{-1} (Figure 2C). The pre-steady-state curves for 8-oxo-dGTP incorporation opposite C and A by T7$^-$ are shown in Figure 2D (the amount of 8-oxo-dGTP available was not sufficient to achieve concentrations above the high K_m of T7$^-$). The rates of the reactions were similar for both 8-oxo-dGTP incorporation opposite C and A (0.72 and 0.64 min^{-1}, respectively).

Steady-State and Pre-Steady-State Kinetics of Next Correct Base Insertion following 8-Oxo-G:C or 8-Oxo-G:A Pairs. Previous pre-steady-state studies of next correct base addition following dNTP incorporation opposite template 8-oxo-G indicated a greater preference for extension past A:8-oxo-G pairs than C:8-oxo-G pairs for all of the four polymerases under consideration (*8*, *9*, *46*). To determine whether DNA polymerases prefer to extend past primer 8-oxo-G:template A base pairs, steady-state and pre-steady-state assays were performed by utilizing a primer containing a 3′ 8-oxo-G annealed to a template containing A or C opposite the modified base. The higher preference for insertion of the next correct base (dCTP) following 8-oxo-G:A pairs by KF$^-$ was defined by a higher insertion efficiency (k_{cat}/K_m) of 69 versus 24 mM^{-1}min^{-1} for insertion of dCTP after the correct base pair (Table 3). Pol II$^-$ showed a higher insertion efficiency for incorporation of dCTP next to the 8-oxo-G:C pair than the 8-oxo-G:A pair (110 vs 17 mM^{-1} min^{-1}). The replicative polymerase HIV-1 RT showed little preference in next base incorporation following 8-oxo-G:A or 8-oxo-G:C base pairs (55 vs 41 mM^{-1} min^{-1}). T7$^-$ had the greatest preference for extension past the mispair (~20-fold) compared to 8-oxo-G:C pairs (330 vs 18 mM^{-1} min^{-1}). The insertion efficiencies for the next correct base addition following 8-oxo-dGTP insertion were greater than 100-fold higher compared to the efficiency of 8-oxo-dGTP incorporation into template DNA for all polymerases studied.

Pre-steady-state reaction progress curves for the next correct base incorporation are shown in Figure 3A−D. KF$^-$, Pol II$^-$, and HIV-1 RT preferred to incorporate the next nucleotide after 8-oxo-G:C pairs, whereas T7$^-$ preferred to incorporate the next correct base after 8-oxo-G:A pairs (Figure 3D). KF$^-$ and HIV-1 RT rates of next base incorporation were low, and no bursts were observed. The rates of KF$^-$ incorporation of dCTP next to 8-oxo-G:C and 8-oxo-G:A pairs were 2.3 and 1.6 min^{-1}, respectively. The rates of HIV-1 RT incorporation of dCTP next to 8-oxo-G:C pairs and 8-oxo-G:A pairs were 1.7 and 1.6 min^{-1}, respectively. Pre-steady-state progress curves of dCTP insertion following 8-oxo-G:C pairs by Pol II$^-$ showed a burst of product formation, with a k_{pol} only 4-fold lower than correct unmodified dNTP incorporation (810 min^{-1}). The rate of dCTP insertion next to 8-oxo-G:A pairs by Pol II$^-$ was 240-fold lower (3.4 min^{-1}) than dCTP insertion adjacent to 8-oxo-G:C pairs (Figure 3B). Pre-steady-state progress

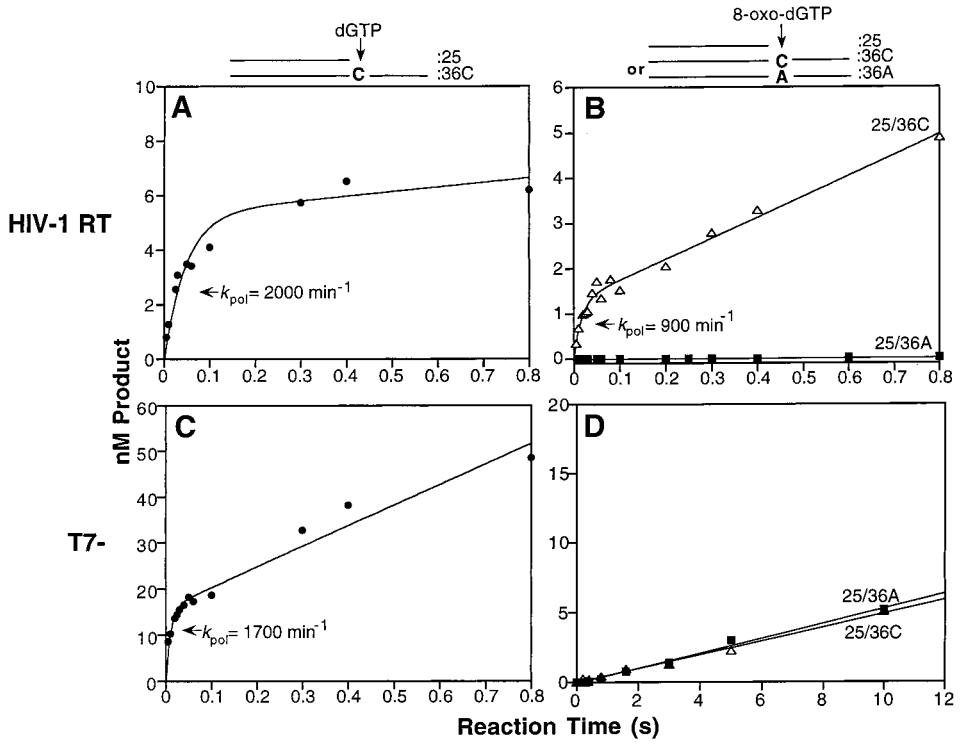

FIGURE 2: Pre-steady-state kinetics of nucleotide incorporation. (A) HIV-1 RT (18 nM) was incubated with 100 nM 24/36C-mer and mixed with a solution of dGTP (220 μM) in the rapid-quench instrument. All reactions were quenched at various times with a final concentration of 0.3 M EDTA (●). (B) HIV-1 RT (36 or 50 nM) was incubated with 100 nM 24/36C-mer (△) or 100 nM 24/36A-mer (■), respectively, mixed with a solution of 8-oxo-dGTP (5 or 2.5 mM, respectively), and quenched at various times with EDTA. (C) T7$^-$ (40 nM) was incubated with 100 nM 24/36C-mer, mixed with a solution of dGTP (220 μM), and quenched at various times with EDTA (●). (D) T7$^-$ (46 nM) was incubated with 100 nM 24/36C-mer (△) or 100 nM 24/36A-mer (■), then mixed with a solution of 8-oxo-dGTP (2.5 mM), and quenched at various times with EDTA.

Table 3: Steady-State Kinetic Parameters of Next Correct Base Insertion following 8-Oxo-dGTP Incorporation

		K_m (mM)	k_{cat} (min^{-1})	k_{cat}/K_m (mM^{-1} min^{-1})[a]
KF$^-$	dCTP → G*:C	0.024 ± 0.009	0.57 ± 0.10	24
	dCTP → G*:A	0.0094 ± 0.0025	0.62 ± 0.05	66
Pol II$^-$	dCTP → G*:C	0.014 ± 0.003	1.6 ± 0.1	110
	dCTP → G*:A	0.031 ± 0.009	0.53 ± 0.07	17
HIV-1 RT	dCTP → G*:C	0.016 ± 0.002	0.65 ± 0.03	41
	dCTP → G*:A	0.0094 ± 0.0039	0.52 ± 0.06	55
T7$^-$	dCTP → G*:C	0.025 ± 0.008	0.44 ± 0.06	18
	dCTP → G*:A	0.054 ± 0.014	18 ± 2	330

[a] Frequency of next correct base insertion (see Table 2)
G* = 8-oxo-dG

curves of dCTP incorporation next to 8-oxo-G:A by T7$^-$ showed a burst of dCTP incorporation with a k_{pol} of 420 min^{-1} (Figure 3D), only 4-fold lower than correct unmodified dNTP incorporation by this enzyme. The rate of T7$^-$ incorporation of dCTP next to 8-oxo-G:C pairs was 950-fold slower than the polymerization rate of next base incorporation after 8-oxo-G:A pairs (0.44 min^{-1}). Figure 3E−F was reproduced from refs *8* and *9* to compare pre-steady-state reactions of the next correct base insertion after template 8-oxo-G base pairs with extension past primer 8-oxo-G pairs in the present study.

K_d Estimation of dGTP and 8-Oxo-dGTP Binding to HIV-1 RT or HIV-1 RT·DNA Complexes. Intrinsic tryptophan fluorescence of HIV-1 RT has been utilized to quantitate interactions of dNTP with HIV-1 RT or HIV-1 RT·dideoxy-terminated primer/template complexes (*43*, *47*). The quenching of enzyme fluorescence by dNTP has been associated with global conformational changes of the enzyme upon dNTP binding and/or quenching of fluorescence in the active site of the enzyme (*43*). The K_d value for binding of dNTP to HIV-1 RT or HIV-1 RT·dideoxy-terminated primer/template complexes determined by fluorescence quenching describes a true thermodynamic equilibrium constant due to the inability of the nucleotide to be incorporated into DNA. The change in fluorescence intensity of HIV-1 RT alone or in the presence of DNA with increasing concentrations of dGTP or 8-oxo-dGTP is shown in Figure 4. The estimated K_d value of 8-oxo-dGTP binding to HIV-1 RT alone (15 ± 4 nM) was not significantly different than the estimated K_d value for dGTP binding (10 ± 2 nM). The dissociation constants for dGTP and 8-oxo-dGTP binding to HIV-1 RT·dideoxy-terminated primer/template complexes (24ddC/36C-mer) were similar to the K_d values of dNTP binding to enzyme alone. The estimated K_d values for dGTP (12 ± 4 nM) and 8-oxo-dGTP (20 ± 6 nM) binding to HIV-1 RT·DNA complexes were also not significantly different.

Apparent kinetic dissociation constants (K_{dapp}) for dNTP binding to HIV-1 RT have previously been estimated by pre-

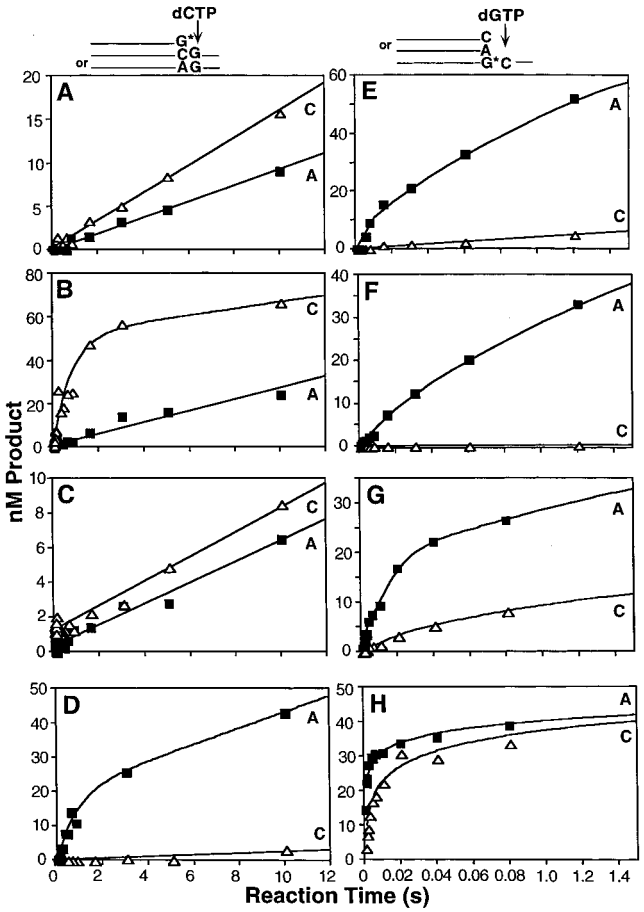

FIGURE 3: (A−D) Pre-steady-state kinetics of the next correct base insertion following 8-oxo-dGTP incorporation. (E−F) Pre-steady-state kinetics of the next correct base insertion following template 8-oxo-G pairs, reproduced from refs *8* and *9*. (A) KF^- (41 nM) was incubated with 100 nM 13/16C-mer (△) or 35 nM KF^- with 100 nM 13/16A-mer (■) and mixed with a solution of dCTP (50 μM) in the rapid-quench instrument. All reactions were quenched after various times with a final concentration of 0.3 M EDTA. (B) Pol II^- (49 nM) was incubated with 100 nM 13/16C-mer (△) or 48 nM Pol II^- with 100 nM 13/16A-mer (■), mixed with a solution of dCTP (50 μM), and quenched at various times with EDTA. (C) HIV-1 RT (49 nM) was incubated with 100 nM 25/36C-mer (△) or 44 nM HIV-1 RT with 100 nM 25/36A-mer (■), mixed with a solution of dCTP (50 μM), and quenched at various times with EDTA. (D) $T7^-$ (37 nM) was incubated with 100 nM 25/36C-mer (△) or 39 nM $T7^-$ with 100 nM 25/36A-mer (■), mixed with a solution of dCTP (100 μM), and quenched at various times with EDTA. (E) KF^- (57 nM) was incubated with 116 nM duplex DNA consisting of a 13-mer unmodified primer with a C (△) or A (■) opposite 8-oxo-G in the 16-mer template (13C/16-mer or 13A/16-mer), mixed with 200 μM dGTP, and quenched at various times with EDTA (*8*). (F) Pol II^- (32 nM) was incubated with 123 nM 13C/16-mer (△) or 13A/16-mer (■), mixed with 200 μM dGTP, and quenched with EDTA at various times (*8*). (G) HIV-1 RT (40 nM) or (H) $T7^-$ (30 nM) was incubated with 102 nM 13C/16-mer (Δ) or 13A/16-mer (■), mixed with 220 μM dGTP, and quenched with EDTA at various times (*9*). G* = 8-oxo-G.

steady-state kinetics (*8*, *9*, *44*) by varying the dNTP concentration and plotting the pre-steady-state burst rates of dNTP incorporation against the dNTP concentration. The K_{dapp} value is a kinetically determined value rather than a thermodynamic equilibrium constant, due to the addition of the nucleotide to the growing primer. Contributions to the K_{dapp} value may also include rates of enzyme conformational change and phosphodiester bond formation as well as rates of dNTP binding. The K_{dapp} value for 8-oxo-dGTP binding

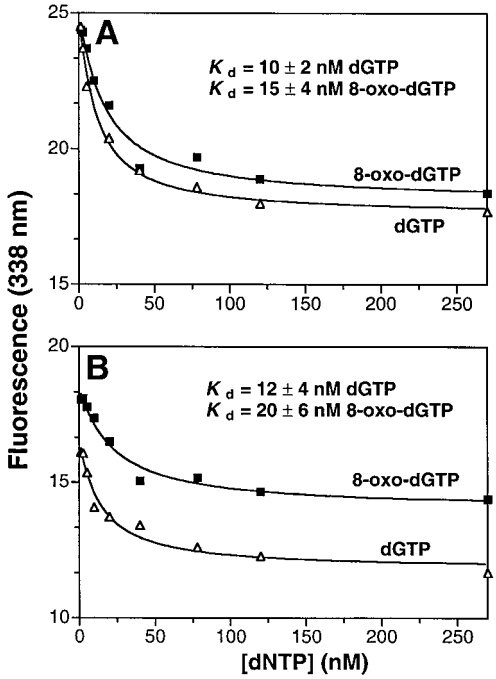

FIGURE 4: (A) K_d estimation of dGTP or 8-oxo-dGTP binding to HIV-1 RT. dGTP or 8-oxo-dGTP (0.0013−1.3 μM) was titrated into a solution of HIV-1 RT (40 nM) and the binding of the dNTP to the enzyme was detected by quenching of fluorescence at 338 nm (excitation at 290 nm). The observed fluorescence intensity was plotted against [dNTP], and the data were fit to a fluorescence quadratic equation (see Experimental Procedures). (B) K_d estimation of dGTP or 8-oxo-dGTP binding to HIV-1 RT·DNA. dGTP or 8-oxo-dGTP (0.0013−1.3 μM) was titrated into a solution of HIV-1 RT (40 nM) and 24/36C-mer with a dideoxy-terminated primer (100 nM) and the binding of the dNTP to the enzyme·DNA was detected by quenching of fluorescence at 338 nm.

(2.3 ± 1.0 mM) was >3 orders of magnitude greater than the pre-steady-state determined dissociation constant for dGTP binding (1.2 ± 1.0 μM) (Figure 5). The K_{dapp} value for dGTP binding was found to be ∼100-fold higher than equilibrium K_d values estimated by fluorescence titrations. The K_{dapp} values for 8-oxo-dGTP binding found in the pre-steady-state experiments were much greater than K_d values estimated from fluorescence titrations (>5 orders of magnitude).

DISCUSSION

In the present study, the incorporation of 8-oxo-dGTP opposite A or C by model DNA polymerases was examined to estimate the potential of this modified triphosphate to be misincorporated and primarily to address the general hypothesis that overall base geometry is the driving force for the fidelity of DNA polymerases. In comparison to normal dGTP incorporation opposite C, 8-oxo-dGTP was found to be a poor substrate for both the repair DNA polymerases KF^- and Pol II^- and the replicative DNA polymerases $T7^-$ and HIV-1 RT. The differences in incorporation of 8-oxo-dGTP compared to dGTP involved lowered insertion efficiencies, lowered k_{cat} and k_{pol} values, and increased K_m values (or increased K_{dapp} values in the case of HIV-1 RT). The differences in the kinetic parameters for 8-oxo-dGTP incorporation, compared to previous studies of normal dNTP incorporation opposite template 8-oxo-G (*8*, *9*), included altered misincorporation frequencies and in preference for

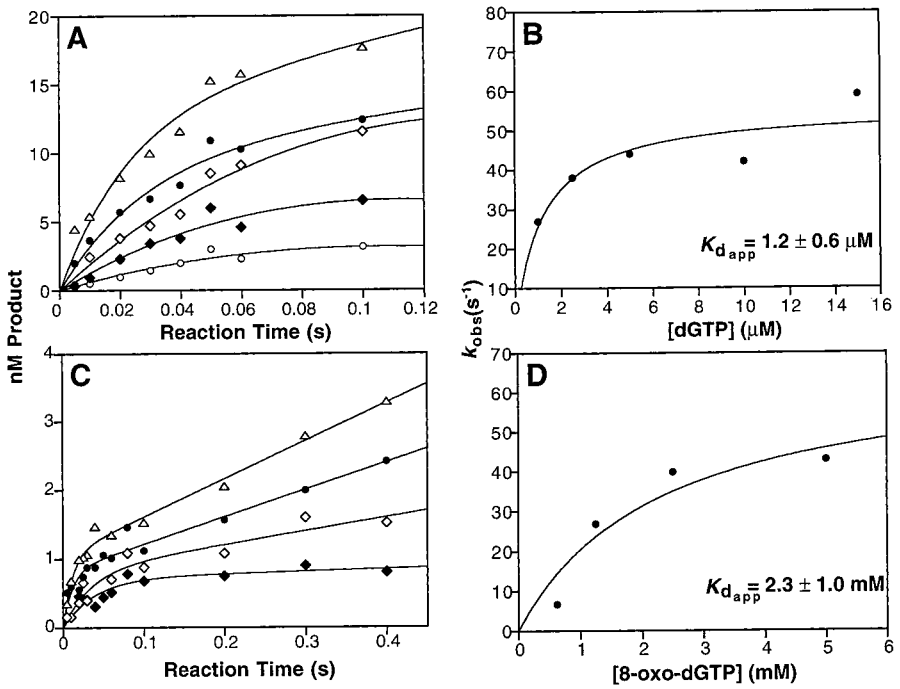

FIGURE 5: (A) dGTP concentration dependence of the pre-steady-state burst rate for HIV-1 RT. HIV-1 RT (55−69 nM) and 100 nM 24/36C-mer were preincubated and then mixed with varying concentrations of dGTP (1 μM, ○; 2.5 μM, ◆; 5 μM, ◇; 10 μM, ●; 15 μM, △). The pre-steady-state rates of product formation were determined by single-exponential analysis of the burst phase as described in the Experimental Procedures. (B) K_{dapp} determination of dGTP binding to HIV-1 RT-DNA by rapid-quench pre-steady-state kinetics. The burst rates from (A) were plotted against [dGTP], and the results were fit to a hyperbola to determine K_{dapp}. (C) 8-oxo-dGTP concentration dependence of the pre-steady-state burst rate for HIV-1 RT. HIV-1 RT (41−61 nM) and 100 nM 24/36C-mer were preincubated and then mixed with varying concentrations of 8-oxo-dGTP (1 mM, ◆; 1.25 mM, ◇; 2.5 mM, ●; 5 mM, △). The pre-steady-state rates of product formation were determined as described above. (D) The burst rates measured with each concentration of 8-oxo-dGTP, were plotted against [8-oxo-dGTP] and the K_{dapp} was determined as described above.

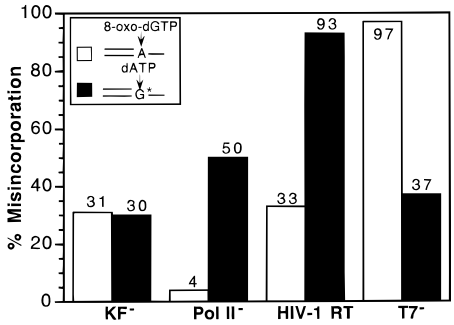

FIGURE 6: Comparison of the percent 8-oxo-dGTP misincorporation ($f/1 + f$) [$f = (k_{cat}/K_m)_{incorrect}/(k_{cat}/K_m)_{correct}$] by KF$^-$, Pol II$^-$, HIV-1 RT, and T7$^-$ to the percent of dATP misincorporation opposite template 8-oxo-G, previously examined in this laboratory by utilizing a complementary primer/template and the same enzymes (*8*, *9*). See Table 2 for definitions. G* = 8-oxo-G.

extension beyond 8-oxo-G:A or 8-oxo-G:C pairs in addition to lowered insertion efficiencies, lowered k_{cat} values, and increased K_m or K_{dapp} values (Figures 3 and 6). Due to the geometrical similarity of 8-oxo-dGTP:A or 8-oxo-dGTP:C and dATP:8-oxo-G or dCTP:8-oxo-G pairs, the differences in DNA polymerase selectivity in these two complementary studies indicate that dNTP incorporation is not based solely upon the overall geometry of Watson−Crick base pairing of 8-oxo-G and reflects the asymmetry of the polymerase active site.

The insertion efficiencies (k_{cat}/K_m) for 8-oxo-dGTP incorporation opposite C by all the enzymes utilized in this study were $>10^4$-fold lower than for normal dGTP incorporation opposite C. The insertion efficiency of 8-oxo-dGTP opposite C ranged from >4 orders of magnitude lower than the correct incorporation of dGTP by HIV-1 RT to >6 orders of magnitude lower by T7$^-$. In comparison to the complementary studies of dNTP incorporation opposite template 8-oxo-G (*8*, *9*), there was more efficient incorporation of unmodified dNTPs opposite template 8-oxo-G than incorporation of 8-oxo-dGTP into unmodified DNA. The difference ranged from 8-fold for the correct incorporation by HIV-1 RT to 37 000-fold for the misincorporation reaction by T7$^-$ (*8*, *9*). The increased efficiency of 8-oxo-dGTP incorporation by HIV-1 RT, compared with the other polymerases, is in accord with the reported lower fidelity of this enzyme (*4*).

The pattern of 8-oxo-dGTP misincorporation opposite template A compared to misincorporation of dATP at template 8-oxo-G adducts differed for all DNA polymerases, with the exception of KF$^-$ (Figure 6). The difference in the percent of misincorporation, depending upon whether 8-oxo-dGTP is the incoming triphosphate or in the template, correlates with other studies in which differences in DNA polymerase fidelity at mispairs were found depending upon whether the nucleotide was in the template or as the incoming triphosphate (*36*−*38*). The differences in misincorporation patterns found previously for studies utilizing KF$^-$ (*38*) and polymerase β (*37*) were relatively small compared with those measured here (Table 2, Figure 6, and refs *8* and *9*). The greater differences in misincorporation frequency for incorporation of 8-oxo-dGTP opposite template A compared to dATP incorporation opposite template 8-oxo-G may be a specific characteristic of this DNA adduct. To our knowledge this study is the first analysis of misincorporation

asymmetry involving modified DNA.

Steady-state kinetic parameters for DNA polymerization can determine the overall selectivity of a DNA polymerase (k_{cat}/K_m); however, the k_{cat} value is a measure of the slowest step in the DNA polymerization reaction (DNA release from the enzyme) and the meaning of K_m is not clear (*4*, *38*). Pre-steady-state kinetics were performed during a single turnover of the enzyme to measure the rate of polymerization (including rates of dNTP binding, conformational change of the enzyme, and phosphodiester bond formation). Pre-steady-state rapid-quench kinetics of normal dGTP incorporation opposite C by the four polymerases studied are shown in Figures 1 and 2. The biphasic nature of the progress curves indicates that the rate-limiting step in the steady state for unmodified nucleotide incorporation occurs after the chemistry step (phosphodiester bond formation). Pre-steady-state studies with most polymerases (all prokaryotic) have demonstrated that the rate-limiting step is at the conformational change step before chemistry for correct dNTP incorporation, but for misincorporations by these enzymes, chemistry is partially rate-limiting (*5*−*7*, *11*, *12*). In pre-steady-state reactions, the chemistry step appears to be partially rate-limiting for DNA polymerization at template 8-oxo-G adducts by KF$^-$, Pol II$^-$, and T7$^-$, with the exception of HIV-1 RT, where chemistry does not appear to be rate-limiting (*8*, *9*). The progress curves of 8-oxo-dGTP incorporation opposite A for all four enzymes were not biphasic, indicating that the overall rate-limiting step for misincorporations in the steady-state reactions is at or before chemistry (Figures 1 and 2). The progress curves for the incorporation of 8-oxo-dGTP opposite C (with the exception of T7$^-$) showed biphasic responses with initial rates of polymerization (k_{pol}) ranging from only 2- to 3-fold lower than unmodified dGTP incorporation by KF$^-$ and HIV-1 RT, to 11-fold lower by Pol II$^-$, indicating that the rate-limiting step in the steady state is after chemistry. The concentrations of 8-oxo-dGTP used in the pre-steady-state were subsaturating for reactions with T7$^-$; therefore the rates of polymerization by T7$^-$ were limited by the amount of substrate. The bursts of incorporation of 8-oxo-dGTP opposite C by KF$^-$, Pol II$^-$, and HIV-1 RT correlated well with the higher insertion efficiency of 8-oxo-dGTP incorporation opposite C in the steady state.

The misincorporation potential of 8-oxo-dGTP appears to be low for the enzymes utilized in these studies. These results, however, do not explain the high mutator phenotype of *mutT*$^-$ strains of *E. coli* (*31*). DNA polymerase fidelity appears to be variable for the enzymes in the present study, and it is, therefore, difficult to predict the efficiency of 8-oxo-dGTP incorporation into DNA by the DNA polymerase system of *E. coli* responsible for replication, polymerase III. The high mutation rate of *mutT*$^-$ strains of *E. coli* may be due to more efficient incorporation of 8-oxo-dGTP by the *E. coli* replicative polymerase III enzyme than found for the model polymerases utilized in this study. In addition, due to the existence of a MutT homologue in humans (*29*), it is of interest to determine whether this 8-oxo-dGTPase is important because of efficient incorporation of 8-oxo-dGTP into DNA by the replicative human DNA polymerase, polymerase δ.

Steady-state incorporation of 8-oxo-dGTP by *E. coli* polymerase III has been examined previously by Maki and Sekiguchi (*32*), who reported smaller differences in the incorporation efficiency of 8-oxo-dGTP compared to normal dNTPs than the differences reported here. This result suggests a greater efficiency of incorporation by the *E. coli* replicative polymerase; however, the K_m values determined for 8-oxo-dGTP by Maki and Sekiguchi (*32*) and others (*48*, *49*) are at least 1 order of magnitude lower than the K_m values determined in this study. The discrepancy in K_m values may be explained in part by the difference in the synthesis of the modified triphosphate. In the previous studies with 8-oxo-dGTP, the 8-oxo-dGTP substrate was directly synthesized and separated from dGTP, as opposed to synthesis from 8-oxo-G. The analysis of purity, as reported in the literature, was not as rigorous. Due to the great difference in insertion efficiency of dGTP and 8-oxo-dGTP, even a small amount of residual dGTP in the reaction ($<0.1\%$) would greatly affect the insertion efficiencies of 8-oxo-dGTP.

In addition to DNA selectivity at dNTP insertion, the extension beyond a DNA adduct can also play an important role in the fidelity of a DNA polymerase. It has been shown that, for template 8-oxo-G adducts, the four DNA polymerases studied here all preferably extend past primer A:template 8-oxo-G pairs more efficiently than primer C:template 8-oxo-G pairs (*8*, *9*, *46*, and Figure 3E−H). In the case of 8-oxo-dGTP, incorporation of this modified base opposite C or A can potentially lead to mutations with subsequent DNA replication. KF$^-$, Pol II$^-$, and HIV-1 RT preferred to extend past primer 8-oxo-G:C base pairs (Figure 3A−C); however, the extension past 8-oxo-G:A or 8-oxo-G:C pairs was generally inefficient for KF$^-$ and HIV-1 RT. Extension past primer 8-oxo-G mispairs occurred efficiently for T7$^-$, with rates of incorporation only 4-fold lower than normal dNTP incorporation into an unmodified template (Figure 2C). These results differed from extension past template 8-oxo-G adducts by T7$^-$, where both A:8-oxo-G and C:8-oxo-G base pairs were efficiently extended (Figure 3H). This study emphasizes the fact that the enzyme active site is asymmetric and maintenance of the overall geometry of the paired bases is not the major influence on fidelity of extension by DNA polymerases.

In the present study, factors governing the rate of polymerization in the pre-steady-state include dNTP binding, enzyme conformational change, and phosphodiester bond formation. To determine whether a DNA polymerase, e.g. HIV-1 RT, selects against 8-oxo-dGTP by its affinity to the enzyme, the dissociation constants (K_d) of 8-oxo-dGTP and dGTP binding were estimated for HIV-1 RT alone and HIV-1 RT·DNA complexes by quenching of intrinsic HIV-1 RT tryptophan fluorescence. There was no difference in affinity of 8-oxo-dGTP binding compared to dGTP binding to HIV-1 RT in the absence of DNA (15 ± 4 vs 10 ± 2 nM) (Figure 4A). The binding affinity of 8-oxo-dGTP or dGTP to HIV-1 RT was not affected by the presence of DNA, indicating that DNA is not a major determinant for initial enzyme dNTP binding selectivity (Figure 4B). These results are in agreement with binding constants determined in previous studies by fluorescence titrations of the correct nucleotide with

HIV-1 RT·terminated primer/template complexes (18 nM) (*47*).[4]

The binding of dNTPs to enzyme·DNA complexes was examined by pre-steady-state rapid-quench kinetics (Figure 5). The kinetic K_{dapp} of 8-oxo-dGTP incorporation opposite C (2.3 mM) was similar to the K_{dapp} for the misincorporation of the normal three dNTPs by HIV-1 RT (~1 mM) (*44*). The K_{dapp} value for normal dGTP incorporation by HIV-1 RT was >3 orders of magnitude less than the apparent dissociation constant for 8-oxo-dGTP binding. In comparison to dCTP incorporation opposite template 8-oxo-G, the K_{dapp} and k_{pol} values for dCTP binding were ~20 and 75-fold lower, respectively, than the values for 8-oxo-dGTP incorporation (*9*). These results suggest that HIV-1 RT selects against 8-oxo-dGTP incorporation opposite C mostly by the affinity of the dNTP to the enzyme (or at least to the conformation of the enzyme directly involved in catalysis; *vide infra*) rather than the actual rate of polymerization, whereas the incorporation of dCTP opposite template 8-oxo-G is influenced more by the rate of polymerization. The selection against 8-oxo-dGTP by most of the polymerases examined (except for KF^-) was influenced more by K_m than k_{cat} (or K_{dapp} for HIV-1 RT).

The observed low K_d values for dNTP binding estimated by fluorescence titrations (thermodynamic equilibrium K_d) indicates that dGTP and 8-oxo-dGTP bind initially with high affinity. The K_d values determined by fluorescence titrations were much lower than K_{dapp} values determined by pre-steady-state kinetics. The large difference between the thermodynamic equilibrium dissociation constant (K_d) and the kinetically determined K_{dapp} indicates that there are contributions to the K_{dapp} such as rates of conformational change after dNTP binding and/or phosphodiester bond formation. The larger difference between the equilibrium K_d and the kinetic K_{dapp} for 8-oxo-dGTP compared to dGTP indicates that the contributions to the K_{dapp} are important for the selectivity of HIV-1 RT against 8-oxo-dGTP. The initial binding of the dNTP may result in productive along with many nonproductive conformations, and as a result the K_d values are low: $K_d = ([E{\cdot}D][dNTP])/([E{\cdot}D{\cdot}dNTP] + [E{\cdot}D{\cdot}dNTP]' + [E{\cdot}D{\cdot}dNTP]'' + ...)$, where E = enzyme and D = DNA. The existence of nonproductive E·D·dNTP conformations is also postulated to explain the less than stoichiometric product formation in the bursts that were observed for 8-oxo-dGTP incorporation (e.g. Figures 1−3 and 5).

We conclude that misincorporation by DNA polymerases is primarily a kinetic as opposed to a thermodynamic event. Misincorporation events must be ultimately understood in the context of the polymerase reaction. These conclusions are consistent with previous studies that showed considerable differences in the patterns of misincorporations for all possible mispairs by different polymerases (*36*−*38*). Although conformations of 8-oxo-G base pairs have been described (*50*−*52*), the structural information cannot be used as the sole guide leading to mispairing events. The misinsertion events are dependent upon whether the modification is in the template or the dNTP. Finally, the practical significance of pools of modified dNTPs and their contribution to mutagenesis is an issue that may depend largely upon the mutagen under consideration.

[4] The much higher K_d values reported by Painter et al. (*43*) are not in accordance with (*47*) or our own results and may be the result of assays using primers capable of elongation.

ACKNOWLEDGMENT

The authors thank Drs. L. L. Furge, S. Langouët, and G. P. Miller and A. N. Mican for helpful suggestions and valuable insights throughout the course of this work. We also gratefully acknowledge S. J. Kambouris for the electrospray mass spectral analysis of 8-oxo-dGTP.

SUPPORTING INFORMATION AVAILABLE

Two figures showing purification of 8-oxo-dGTP by SAX- and DEAE-HPLC and characterization of 8-oxo-dGTP by electrospray mass spectral analysis (3 pages). Ordering information is given on any current masthead page.

REFERENCES

1. Bonner, C. A., Randall, S. R., Rayssiguier, C., Radman, M., Eritia, R., Kaplan, B. E., McEntee, K., and Goodman, M. F. (1988) *J. Biol. Chem. 263*, 18946−18952.
2. Escarcellar, M., Hicks, J., Gudmundsson, G., Trump, G., Touati, D., Lorett, S., Foster, P., McEntee, K., and Goodman, M. F. (1994) *J. Bacteriol. 176*, 6221−6228.
3. Rangarajan, S., Gudmundsson, G., Qiu, Z., Foster, P. L., and Goodman, M. F. (1997) *Proc. Natl. Acad. Sci. U.S.A. 94*, 946−951.
4. Johnson, K. A. (1993) *Annu. Rev. Biochem. 62*, 685−713.
5. Kuchta, R. D., Mizrahi, V., Benkovic, P. A., Johnson, K. A., and Benkovic, S. J. (1987) *Biochemistry 26*, 8410−8417.
6. Reardon, J. E. (1992) *Biochemistry 31*, 4473−4479.
7. Patel, S. S., Wong, I., and Johnson, K. A. (1991) *Biochemistry 30*, 511−525.
8. Lowe, L. G., and Guengerich, F. P. (1996) *Biochemistry 35*, 9840−9849.
9. Furge, L. L., and Guengerich, F. P. (1997) *Biochemistry 36*, 6475−6487.
10. Tan, H. B., Swann, P. F., and Chance, E. M. (1994) *Biochemistry 33*, 5335−5346.
11. Eger, B. T., and Benkovic, S. J. (1992) *Biochemistry 31*, 9227−9236.
12. Wong, I., Patel, S. S., and Johnson, K. A. (1991) *Biochemistry 30*, 526−537.
13. Ames, B. N., and Gold, L. S. (1991) *Mutation Res. 250*, 3−16.
14. Kasai, H. and Nishimura, S. (1991) in *Oxidative Stress, Oxidants, and Antioxidants* (Sies, H., Ed.) pp 99−116, Academic Press, London.
15. Shibutani, S., Takeshita, M., and Grollman, A. P. (1991) *Nature 349*, 431−434.
16. Moriya, M., Ou, C., Bodepudi, V., Johnson, F., Takeshita, M., and Grollman, A. P. (1991) *Mutation Res., DNA Repair 254*, 281−288.
17. Cheng, K. C., Cahill, D. S., Kasai, H., Nishimura, S., and Loeb, L. A. (1992) *J. Biol. Chem. 267*, 166−172.
18. Klein, J. C., Bleeker, M. J., Saris, C. P., Roelen, H. C. P. F., Brugghe, H. F., van den Elst, H., van der Marel, G. A., van Boom, J. H., Westra, J. G., Kriek, E., and Berns, A. J. M. (1992) *Nucl. Acids Res. 20*, 4437−4443.
19. Le Page, F., Margot, A., Grollman, A. P., Sarasin, A., and Gentil, A. (1995) *Carcinogenesis 16*, 2779−2784.
20. Kamiya, H., Murata-Kamiya, N., Koizume, S., Inoue, H., Nishimura, S., and Ohtsuka, E. (1995) *Carcinogenesis 16*, 883−889.
21. Kasai, H., Crain, P. F., Kuchino, Y., Nishimura, S., Ootsuyama, A., and Tanooka, H. (1986) *Carcinogenesis 7*, 1849−1851.
22. Shigenaga, M. K., Gimeno, C. J., and Ames, B. N. (1989) *Proc. Natl. Acad. Sci. U.S.A. 86*, 9697−9701.
23. Michaels, M. L., and Miller, J. H. (1992) *J. Bacteriol. 174*, 6321−6325.
24. Michaels, M. L., Pham, L., Cruz, C., and Miller, J. H. (1991) *Nucl. Acids Res. 19*, 3629−3632.

25. Chung, M. H., Kasai, H., Jones, D. S., Inoue, H., Ishikawa, H., Ohtsuka, E., and Nishimura, S. (1991) *Mutation Res. 254*, 1−12.
26. Tchou, J., Kasai, H., Shibutani, S., Chung, M. H., Laval, J., Grollman, A. P., and Nishimura, S. (1991) *Proc. Natl. Acad. Sci. U.S.A. 88*, 4690−4694.
27. Michaels, M. L., Cruz, C., Grollman, A. P., and Miller, J. H. (1992) *Proc. Natl. Acad. Sci. U.S.A. 89*, 7022−7025.
28. Nghiem, Y., Cabrera, M., Cupples, C. G., and Miller, J. H. (1988) *Proc. Natl. Acad. Sci. U.S.A. 85*, 2709−2713.
29. Sakumi, K., Furuichi, M., Tsuzuki, T., Kakuma, T., Kawabata, S.-I., Maki, H., and Sekiguchi, M. (1993) *J. Biol. Chem. 268*, 23524−23530.
30. Bhatnagar, S. K., and Bessman, M. J. (1988) *J. Biol. Chem. 263*, 8953−8957.
31. Tajiri, T., Maki, H., and Sekiguchi, M. (1995) *Mutation Res. 336*, 257−267.
32. Maki, H., and Sekiguchi, M. (1992) *Nature 355*, 273−275.
33. Pavlov, Y. I., Minnick, D. T., Izuta, S., and Kunkel, T. A. (1994) *Biochemistry 33*, 4695−4701.
34. Inoue, M., Kamiya, H., Fujikawa, K., Ootsuyama, Y., Murata-Kamiya, N., Osaki, T., Yasumoto, K., and Kasai, H. (1998) *J. Biol. Chem. 273*, 11069−11074.
35. Goodman, M. F. (1997) *Proc. Natl. Acad. Sci. U.S.A. 94*, 10493−10495.
36. Kunkel, T. A., and Bebenek, K. (1988) *Biochim. Biophys. Acta 951*, 1−15.
37. Ahn, J., Werneburg, B. G., and Tsai, M. D. (1997) *Biochemistry 36*, 1100−1107.
38. Carroll, S. S., Cowart, M., and Benkovic, S. J. (1991) *Biochemistry 30*, 804−813.
39. Bodepudi, V., Shibutani, S., and Johnson, F. (1992) *Chem. Res. Toxicol. 5*, 608−617.
40. Ludwig, J. (1981) *Acta Biochim. Biophys. Acad. Sci. Hung. 16*, 131−133.
41. Kasai, H., and Nishimura, S. (1984) *Nucl. Acids Res. 12*, 2137−2145.
42. Borer, P. N. (1975) in *Handbook of Biochemistry and Molecular Biology*, (Fasman, G. D., Ed.) 3rd ed., pp 589−590, CRC Press, Cleveland, OH.
43. Painter, G. R., Wright, L. L., Hopkins, S., and Furman, P. A. (1991) *J. Biol. Chem. 266*, 19362−19368.
44. Kati, W. M., Johnson, K. A., Jerva, L. F., and Anderson, K. S. (1992) *J. Biol. Chem. 267*, 25988−25997.
45. Boosalis, M. S., Mosbaugh, D. W., Hamatake, R., Sugino, A., Kunkel, T. A., and Goodman, M. F. (1989) *J. Biol. Chem. 264*, 11360−11366.
46. Furge, L. L., and Guengerich, F. P. (1998) *Biochemistry 37*, 3567−3574.
47. Rittinger, K., Divita, G., and Goody, R. S. (1995) *Proc. Natl. Acad. Sci. U.S.A. 92*, 8046−8049.
48. Purmal, A. A., Kow, Y. W., and Wallace, S. S. (1994) *Nucl. Acids Res. 22*, 3930−3935.
49. Kamath-Loeb, A. S., Hizi, A., Kasai, H., and Loeb, L. A. (1997) *J. Biol. Chem. 272*, 5982−5898.
50. Gannett, P. M., and Sura, T. P. (1993) *Chem. Res. Toxicol. 6*, 690−700.
51. Kouchakdjian, M., Bodepudi, V., Shibutani, S., Eisenberg, M., Johnson, F., Grollman, A. P., and Patel, D. J. (1991) *Biochemistry 30*, 1403−1412.
52. Oda, Y., Uesugi, S., Ikehara, M., Nishimura, S., Kawase, Y., Ishikawa, H., Inoue, H., and Ohtsuka, E. (1991) *Nucl. Acids Res. 19*, 1407−1412.

BI981346D